Asian Journal of Chemistry; Vol. 25, No. 14 (2013), 7937-7940

ASIAN JOURNAL OF CHEMISTRY

http://dx.doi.org/10.14233/ajchem.2013.14739

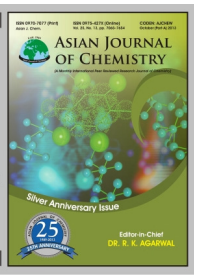

Structural and Electrochemical Studies on Tavorite Crystal $LiFePO_4F$ Synthesized by Sol-Gel Process

FENGCHAO WANG[1], GUANGJIN ZHAO[1,*], WENLONG WU[1] and BIN HUANG[2]

[1]HAEPC Electric Power Research Instititute, Zhengzhou 450052, P.R. China
[2]College of Chemistry and Chemical Engineering, Central South University, Changsha 410083, P.R. China

*Corresponding author: E-mail: zgj5251214@163.com; wangfc1986@163.com

(*Received*: 25 October 2012; *Accepted*: 27 July 2013) AJC-13844

$LiFePO_4F$ as a cathode material for Li-ion (Li^+) batteries is prepared by a novel sol-gel process followed by calcinations. The obtained crystalline powder is isostructural with amblygonite and tavorite, adopting a triclinic $P\bar{1}$ space group that can apply a three-dimensional (3D) channel system for Li^+ insertion/extraction. The particle size of the obtained material is 300-500 nm. The diffusion coefficient of the as-prepared sample, studied by electrochemical impedance spectroscopy (EIS), is higher than that of raw $LiFePO_4$ by three orders of magnitude, which confirms the fast Li^+ migration in this material. The galvanostatic discharge-charge capacity is 145 mAh g^{-1}, which is close to the theoretical capacity of 152 mAh g^{-1}. Furthermore, the cyclic performance is excellent as well.

Key Words: Energy storage and conversion, Tavorite, Sol-gel preparation, Lithium ion batteries.

INTRODUCTION

In the past decade, considering the cost and safety issues, the new-generation cathode materials based on polyanion compounds (*e.g.*, $LiFePO_4$) have been suggested as a candidate rather than $LiCoO_2$ in large-scale applications such as electric vehicles (EVs), hybrid electric vehicles (HEVs) and intelligent power stations[1,2]. In order to meet the demands of such applications, many novel technologies for increasing Li^+ diffusivity and conductivity of the cathode materials are developed. In recent years, the family of alkali-metal transition-metal fluoro(hydroxyl) phosphates/fluorosulfates has been interesting researchers owing to their 3D framework which can apply a fast-migration channel system for Li^+. For instance, it was reported that $LiZnSO_4F$ with a 3D structure framework was adequate for a ceramic electrolyte[3] and the ferrous homologue $LiFeSO_4F$ and $NaFeSO_4F$ were reported as intriguing electrode materials[4,5] with obvious advantages such as low toxicity and high Li^+ diffusivity. However, $LiFeSO_4F$ is a metastable crystal due to the solubility of SO_4^{2-}. For $LiMSO_4F$ (M = Fe, Co, Ni), first-principle calculations result showed that significant electron-charge transfer may occur on the oxygen anions with Li^+ extraction can lead to structural and thermal instabilities[6].

On the contrary, the analogues based on PO_4F^{4-} polyanion were reported to be much more stable[7-11]. The results, obtained by Ramesh *et al.*[7] proved that the lithium iron fluorophosphates $LiFePO_4F$ was an adequate material for the prospective applications of Li^+ batteries due to its facile Li^+ transfer without a strict control of particle size or coating conductors. However, to best of knowledge any modification of $LiFePO_4F$ has not been studied. Thus, the exploration work of $LiFePO_4F$ is necessary.

In this paper, finer $LiFePO_4F$ powder with a narrow size distribution was obtained by a novel sol-gel process followed by heat treatments and the diffusion coefficient was calculated based on the electrochemical impedance spectroscopy (EIS) result. Besides, the galvanostatic discharge-charge and cyclic performance were implemented as well.

EXPERIMENTAL

The $LiFePO_4F$ was synthesized by the sol-gel route described below. Stoichiometric quantities of ferrous sulfate and orthophosphoric acid were dissolved in deionized water to form light green solution. Hydrogen peroxide was dripped in the solution in order to oxide the Fe^{2+}-Fe^{3+} and then the solution changed into yellow suspension. Subsequently oxalic acid was added and the suspension was clear again. The pH value was adjusted to 7 followed by mixing CH_3COOLi and NH_4F. The final suspension contained Li/Fe/P/F in a 1:1:1:1 ratio was dried in an oil bath at 80 ºC with magnetic stirring overnight. The obtained yellow-green xerogel was putted in a muffle furnace at 350 ºC for 5 h, followed by calcination at 550 ºC in air for 2 h, then the final powder was obtained after grinding. In our experiments, $Li_3Fe_2(PO_4)_3$ was obtained in our trial guided by the route proposed by Barker *et al.*[12].

X-Ray diffraction (XRD) patterns were measured using a JapanD/max2550 diffractometer (CuK_α, 1.54178 Å) under a 40 kV potential and 300 mA current. The diffraction data were collected at step mode over the angular range of 10-80º with a step size 0.02º. The scanning electron microscope (SEM) images were obtained by a JSM-6360LV scanning electron microscope.

For electrochemistry studies, the as-prepared $LiFePO_4F$ was grinded with acetylene black (super P) for 20 min. Then, the mixture was blended with poly(tetrafluoroethylene) (PTFE) to form a lump of paste followed by pressing onto aluminum foil and dried at 110 ºC overnight in a vacuum oven, the weight ratio of the sample, super P and PTFE was 80:10:10, The loading amount of active material was 5 mg cm^{-2}. Afterwards, the CR2016 coin cell with a metallic lithium anode was assembled in a glove box (M BRAUN, Germany) under Ar with O_2 and H_2O lower than 10 ppm. The electrochemical impedance spectroscopy (EIS) measurement was conducted by Parstat 2273 electrochemical working station (America), with a frequency range of 10 mHz to 100 kHz and an excitation amplitude of 5 mV. For investigating the charging and discharging performance, cells were cycled between 1.8 and 4.2 V in the galvanostatic mode using a Land CT2001C cell test system (Wuhan, China) at room temperature.

RESULTS AND DISCUSSION

The X-ray diffraction (XRD) pattern for the as-prepared $LiFePO_4F$, shown in Fig. 1a, indicates the single phase of $LiFePO_4F$ with trace quantity of $Li_3Fe_2(PO_4)_3$ as impurity. The obtained crystalline powder is adopts triclinic $P\bar{1}$ space group with the lattice parameters are: a = 5.34023 Å, b = 7.24818 Å, c = 5.07321 Å, α = 108.5199º, β = 98.2166º, γ = 106.7507º, V = 172.2 $Å^3$. The result in this paper is homologous to that of the tavorite $LiFePO_4(OH)$ obtained by Marx *et al.*[8], which demonstrates the isostructuralism between $LiFePO_4F$ and $LiFePO_4(OH)$. Fig. 1b illustrates the structure of $LiFePO_4F$, it can be seen that Li^+ can insert/extract (labeled 'Li-ions I/E' in the drawing) along a, b and c axes. This 3D channel system could lead to a high Li^+ diffusion coefficient, which has confirmed by electrochemical impedance method stated below. Fig. 1c shows the SEM images of the as-prepared powder at a magnification of 20,000-fold. The dimensions of the particles are *ca.* 300-500 nm.

Electrochemical impedance spectroscopy result (Fig. 2a) can investigate the kinetic properties of $LiFePO_4F$. Before the test, the half-cell was charged to 2.8 V. The Nyquist plot is composed of a semicircle in high frequency region and a tail in low frequency one. The equivalent circuit is showed in the inset of Fig. 2a. The ohmic resistance (R_s) of the electrolyte and electrode is equal to the intercept at the Z_{re} axis. The charge transfer resistance (R_{ct}) is indicated by the radius of the semicircle in the middle frequency range. And the Warburg impedance (Z_w), represented by the low frequency tail, is associated with Li^+ diffusion in the material particles[13]. From EIS result, the diffusion coefficient of Li^+ in the $LiFePO_4F$ particles can be calculated.

The Li^+ diffusion coefficient is calculated according to the following equations[14]:

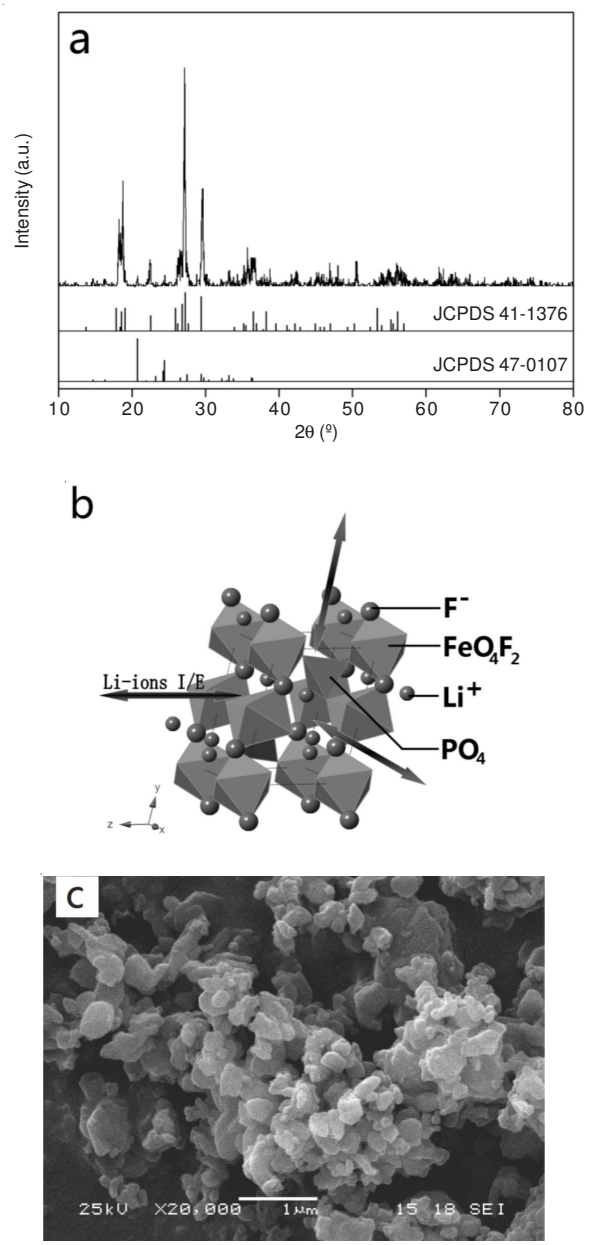

Fig. 1. (a) XRD pattern of as-prepared $LiFePO_4F$ and its structure (inset). (b) Scanning electron microscope (SEM) patterns of $LiFePO_4F$. (c) The structure of $LiFePO_4F$ and its pathway for Li^+ insertion/extraction

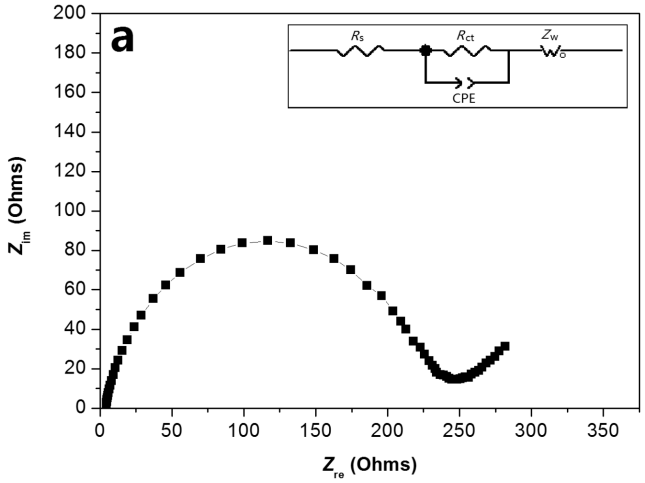

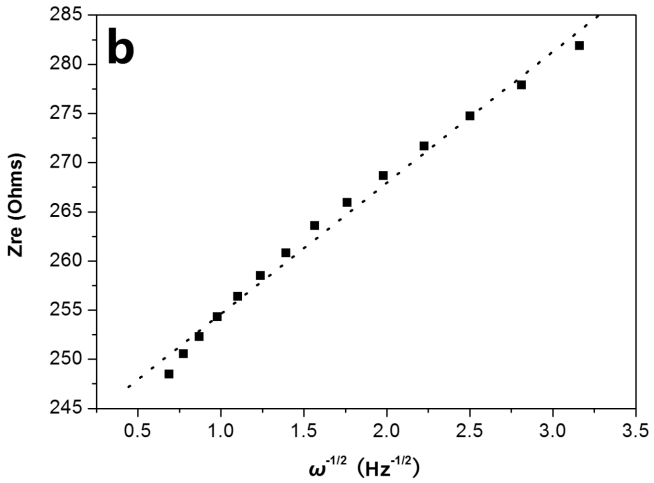

Fig. 2. (a) Nyquist plot of $LiFePO_4F$ at 2.8 V and the equivalent circuit (inset). (b) Z_{re}-$\omega^{-1/2}$ plot derived from the low frequency tail of the Nyquist plot

$$D = R^2T^2 \times (2A^2n^4F^4C^2\sigma^2)^{-1} \quad (1)$$

$$Z_{re} = R_s + R_{ct} + \sigma\omega^{-1/2} \quad (2)$$

where in the eqn. 1, D is diffusion coefficient of Li^+, R is the gas constant, T is the absolute temperature, A is the surface area of the cathode, n is the number of electrons per molecule during oxidization, F is the Faraday constant, C is the concentration of Li^+ and σ is the Warburg factor which is related with Z_{re}, shown in eqn. 2.

In our experiment, the electrodes are pressed on round aluminum foils with the diameter of 10 mm, so the value of A is 0.785 cm^2. According to the structure analysis before, the calculated value of C is 1.928×10^{-2} mol cm^{-3}. The σ can be obtained from the Z_{re}-$\omega^{-1/2}$ plot, which is shown in Fig. 2b. From the linear fit of the dots (dotted line), the derived value of σ is 13.33. Therefore, the D is 8.71×10^{-13} cm^2 s^{-1}. Comparison of the D between $LiFePO_4F$ (obtained in our experiment) and $LiFePO_4$ (synthesized by Liu *et al.*[15]) is listed in Table-1. It can be seen that the D of $LiFePO_4F$ without modification is higher than that of raw $LiFePO_4$ by three orders of magnitude and in the same range of magnitude with $LiFePO_4$/C (covered with 10 wt %).

TABLE-1
COMPARISON OF D_{Li^+} BETWEEN AS-PREPARED $LiFePO_4F$ AND $LiFePO_4$ OBTAINED BY LIU *et al.*[15]

Cathode materials	Modifications	Li^+ diffusion coefficient (D) (cm^2 s^{-1})
$LiFePO_4F$	None	8.71×10^{-13}
$LiFePO_4$	None	9.98×10^{-16}
$LiFePO_4$/C	Covered with 5 wt % carbon	1.01×10^{-13}
$LiFePO_4$/C	Covered with 10 wt % carbon	9.20×10^{-13}
$LiFePO_4$/C	Covered with 20 wt % carbon	4.89×10^{-12}

The result of galvanostatic discharge-charge performance (1/10 C) is shown in Fig. 3a. The curve shows a specific capacity of *ca.* 145 mAh g^{-1} and a pair of flat plateaus at *ca.* 2.8 V indicates a facile Li^+ intercalation for $LiFePO_4F$. This is identical to that of other groups[7,11]. The inset of Fig. 3a is the differential capacity *versus* voltage plot derived from the discharge-charge profile. A couple of peaks show the discharging

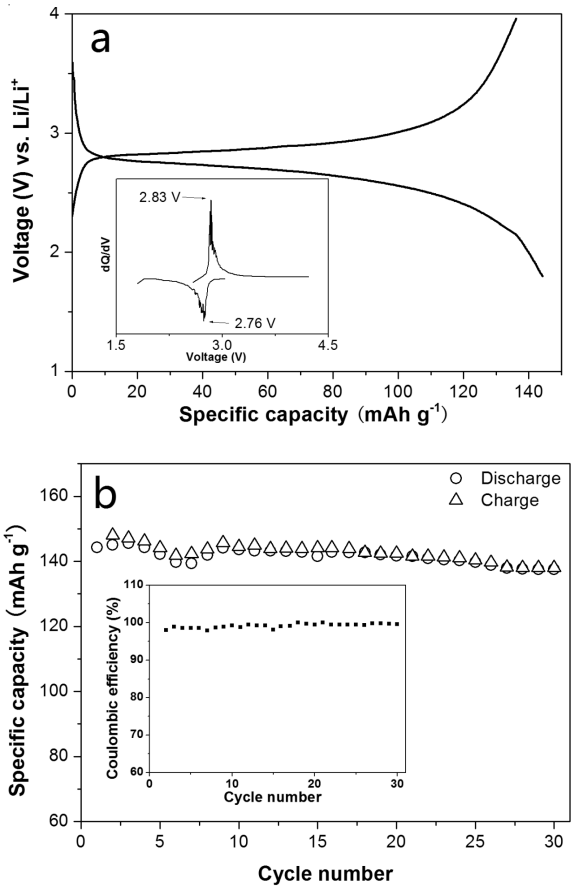

Fig. 3. (a) Discharge-charge curve at 1/10 C and the corresponding differential capacity *versus* voltage plot (inset). (b) Cyclic performance of $LiFePO_4F$ in the galvanostatic mode and the corresponding coulombic efficiency (inset)

and charging plateaus at 2.76 and 2.83 V, respectively. The narrow peak separation (0.07 V) indicates that the overpotential on Li^+ insertion/extraction is fairly low. Fig. 3b shows the cyclic performance of the as-prepared $LiFePO_4F$. It can be known that the capacity is stable in 30 cycles. After 30 cycles, the material exhibits discharge capacity of *ca.* 140 mAh g^{-1}, indicating a good sustainability. The coulombic efficiencies, shown in the inset of Fig. 3b, are almost above 95 %, indicating the reversibility of the $LiFePO_4F$-Li_2FePO_4F transformation.

Conclusion

Tavorite $LiFePO_4F$ crystalline powder is successfully synthesized through a novel sol-gel process followed by heat treatments and we firstly derived the Li^+ diffusion coefficient in this material from the EIS result. The result further confirms the high ionic conductivity of $LiFePO_4F$. The discharge-charge curves and cyclic properties show that the as-prepared material exhibits an excellent electrochemical activity, high redox reversibility and sustainable capacity. As a new cathode material for Li^+ batteries, the prospect of $LiFePO_4F$ and the tavorite-type materials is certainly alluring due to its excellent performance.

ACKNOWLEDGEMENTS

This work was financially supported by the Scientific Research project of State Grid Corporation of China (No. 1213).

REFERENCES

1. J.M. Tarascon and M. Armand, *Nature*, **414**, 359 (2001).
2. J. Ma, B.H. Li, H.D. Du, C.J. Xu and F.Y. Kang, *J. Solid State Electrochem.*, **16**, 1353 (2012).
3. P. Barpanda, J.N. Chotard, C. Delacourt, M. Reynaud, Y. Filinchuk, M. Armand, M. Deschamps and J.M. Tarascon, *Angew. Chem. Int. Ed.*, **50**, 2526 (2011).
4. N. Recham, J.N. Chotard, L. Dupont, C. Delacourt, W. Walker, M. Armand and J.M. Tarascon, *Nature Mater.*, **9**, 68 (2009).
5. R. Tripathi, T.N. Ramesh, B.L. Ellis and L.F. Nazar, *Angew. Chem. Int. Ed.*, **49**, 8738 (2010).
6. Y. Cai, G. Chen, X. Xu, F. Du, Z. Li, X. Meng, C. Wang and Y. Wei, *J. Phys. Chem. C*, **115**, 7032 (2011).
7. T.N. Ramesh, K.T. Lee, B.L. Ellis and L.F. Nazar, *Electrochem. Solid-State Lett.*, **13**, A43 (2010).
8. N. Marx, L. Croguennec, D. Carlier, A. Wattiaux, F.L. Cras, E. Suard and C. Delmas, *Dalton Transc.*, **39**, 5108 (2010).
9. M.V. Reddy, G.V. Subba, Rao and B.V.R. Chowdari, *J. Power Sources*, **195**, 5768 (2010).
10. X. Qiao, J. Yang, Y. Wang, Q. Chen, T. Zhang, L. Liu and X. Wang, *J. Solid State Electrochem*, 16, 1211 (2012).
11. N. Recham, J.N. Chotard, J.C. Jumas, L. Laffont, M. Armand and J.M. Tarascon, *Chem. Mater.*, **22**, 1142 (2010).
12. J. Barker, M. Saidi and J. Swoyer, US Pat, 6855462 B2 (2002).
13. X. Yin, K. Huang, S. Liu, H. Wang and H. Wang, *J. Power Sources*, **195**, 4308 (2010).
14. A. Bard, L. Faulkner, Electrochemical Methods, Wiley, New York, edn. 2, p. 231 (2001).
15. H. Liu, C. Li, H.P. Zhang, L.J. Fu, Y.P. Wu and H.Q. Wu, *J. Power Sources*, **159**, 717 (2006).